ArXiv:astro-ph, Nov 9-13, 2015

От Сильченко О.К.

Astro-ph: 1511.02862

SATELLITE QUENCHING AND GALACTIC CONFORMITY AT $0.3 < Z < 2.5$ *

Lalitwadee Kawinwanichakij[1†], Ryan F. Quadri[1,2], Casey Papovich[1], Glenn G. Kacprzak[3], Ivo Labbé[4], Lee R. Spitler[5,6], Caroline M. S. Straatman[4], Kim-Vy H. Tran[1], Rebecca Allen[3,6], Peter Behroozi[7], Michael Cowley[5], Avishai Dekel[8], Karl Glazebrook[3], W. G Hartley[9,10], Daniel D. Kelson[11], David C. Koo[12], Seong-Kook Lee[13], Yu Lu[11], Themiya Nanayakkara[3], S. Eric Persson[11], Joel Primack[12], Vithal Tilvi[1], Adam R. Tomczak[1], and Pieter van Dokkum[14]

Draft Version Nov 9, 2015

ABSTRACT

We measure the evolution of the quiescent fraction and quenching efficiency of satellites around star-forming and quiescent central galaxies with stellar mass $\log(M_{\rm cen}/{\rm M}_{\odot}) > 10.5$ at $0.3 < z < 2.5$. We combine imaging from three deep near-infrared-selected surveys (ZFOURGE/CANDELS, UDS, and UltraVISTA), which allows us to select a stellar-mass complete sample of satellites with $\log(M_{\rm sat}/{\rm M}_{\odot}) > 9.3$. Satellites for both star-forming and quiescent central galaxies have higher quiescent fractions compared to field galaxies matched in stellar mass at all redshifts. We also observe "galactic conformity": satellites around quiescent centrals are more likely to be quenched compared to the satellites around star-forming centrals. In our sample, this conformity signal is significant at $\gtrsim 3\sigma$ for $0.6 < z < 1.6$, whereas it is only weakly significant at $0.3 < z < 0.6$ and $1.6 < z < 2.5$. Therefore, conformity (and therefore satellite quenching) has been present for a significant fraction of the age of the universe. The satellite quenching efficiency increases with increasing stellar mass of the central, but does not appear to depend on the stellar mass of the satellite to the mass limit of our sample. When we compare the satellite quenching efficiency of star-forming centrals with stellar masses 0.2 dex higher than quiescent centrals (which should account for any difference in halo mass), the conformity signal decreases, but remains statistically significant at $0.6 < z < 0.9$. This is evidence that satellite quenching is connected to the star-formation properties of the central as well as to the mass of the halo. We discuss physical effects that may contribute to galactic conformity, and emphasize that they must allow for continued star-formation in the central galaxy even as the satellites are quenched.

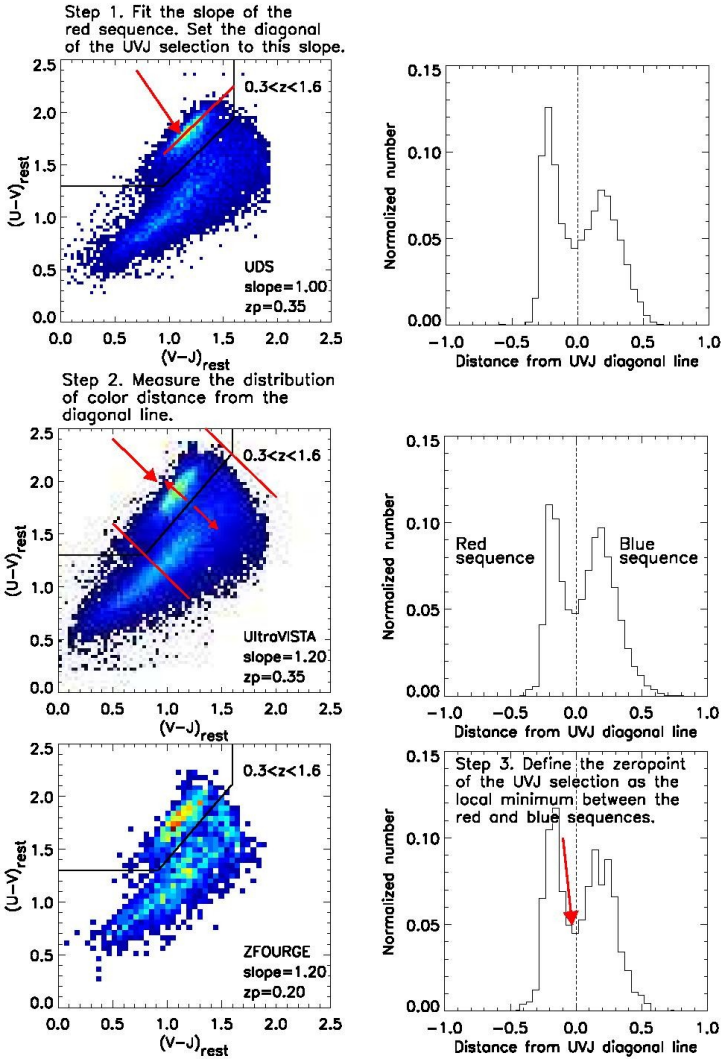

Figure 2. *Left*: Rest-frame $U-V$ versus $V-J$ color for galaxy sample with $\log(M_*/\mathrm{M}_\odot) > 9.8$ at $0.3 < z < 1.6$. The galaxies in the upper left region of the plot (separated by the solid line) are quiescent; galaxies outside this region are star forming. *Right*: Distribution of the distance (in color) from the diagonal line in UVJ color (the slope A, see Equation 1) that separates the quiescent and star-forming sequences in the UVJ color space. We define the zeropoint of the UVJ quiescent region as the local minimum in this distribution, indicated by the vertical dashed line.

Жизнь спутника зависит от хозяина!

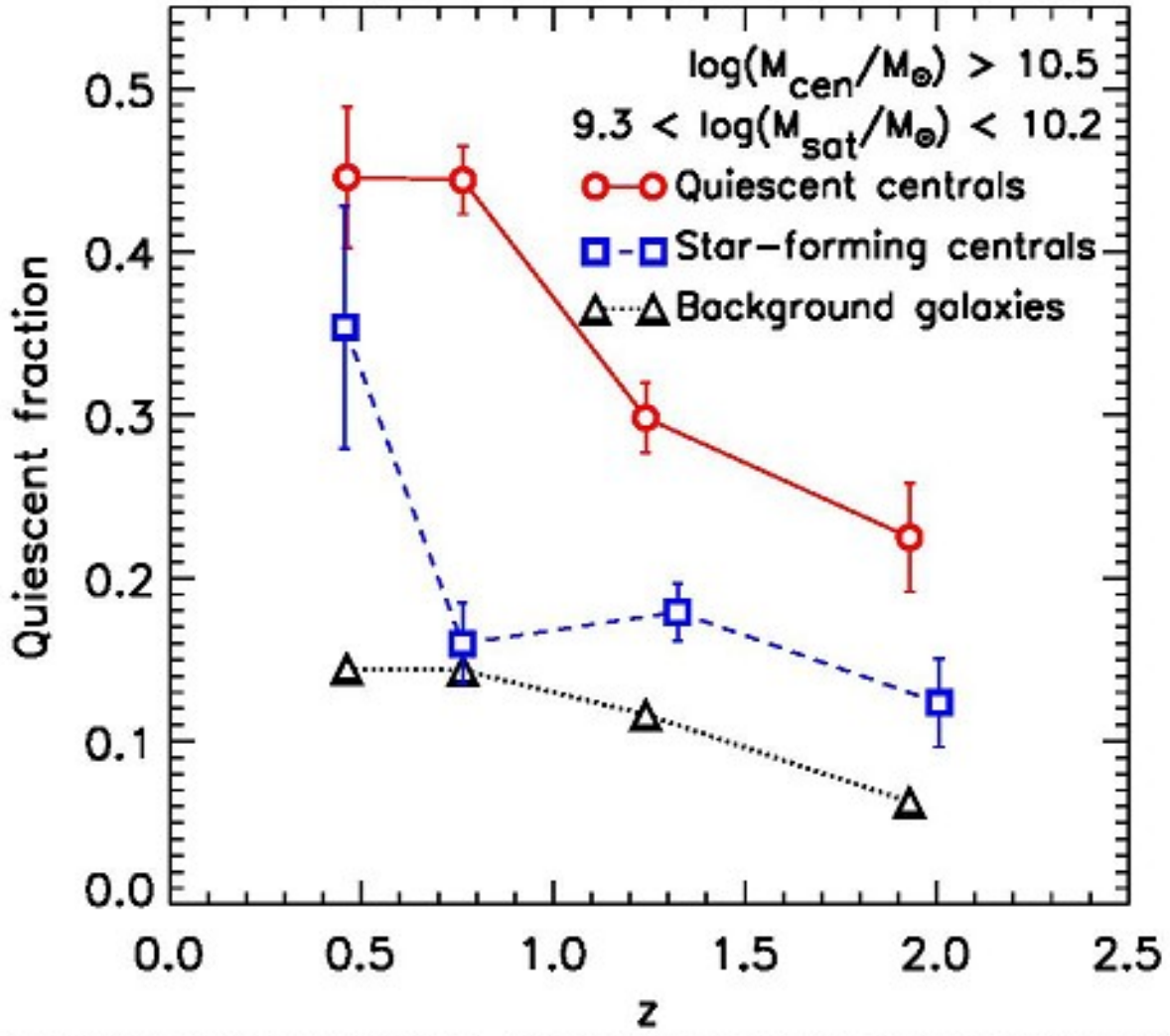

Figure 6. The average quiescent fraction of satellites ($f_{q,sat}$) with stellar mass of $9.3 < \log(M_{sat}/M_{\odot}) < 10.2$ around quiescent centrals (red circles) and star-forming centrals (blue squares) with stellar mass of $\log(M_{cen}/M_{\odot}) > 10.5$ combining from the three datasets. The average quiescent fraction of background galaxies of the same stellar masses are also shown (black triangles).

Astro-ph:1511.03264

The AIMSS Project III: The Stellar Populations of Compact Stellar Systems

Joachim Janz[1⋆], Mark A. Norris[2,3], Duncan A. Forbes[1], Avon Huxor[4], Aaron J. Romanowsky[5,6], Matthias J. Frank[7], Carlos G. Escudero[8,9,10], Favio R. Faifer[8,9,10], Juan Carlos Forte[10,11], Sheila J. Kannappan[12], Claudia Maraston[13], Jean P. Brodie[6], Jay Strader[14], Bradley R. Thompson[5]

[1] *Centre for Astrophysics & Supercomputing, Swinburne University, Hawthorn, VIC 3122, Australia*
[2] *Max Planck Institut für Astronomie, Königstuhl 17, D-69117, Heidelberg, Germany*
[3] *Jeremiah Horrocks Institute, University of Central Lancashire, Preston, PR1 2HE, United Kingdom*
[4] *Astronomisches Rechen-Institut, Zentrum für Astronomie der Universität Heidelberg, Mönchstraße 12-14, D-69120 Heidelberg, Germany*
[5] *Department of Physics and Astronomy, San José State University, One Washington Square, San Jose, CA 95192, USA*
[6] *University of California Observatories, 1156 High Street, Santa Cruz, CA 95064, USA*
[7] *Landessternwarte, Zentrum für Astronomie der Universität Heidelberg, Königsstuhl 12, D-69117 Heidelberg, Germany*
[8] *Facultad de Cs. Astronómicas y Geofísicas, UNLP, Paseo del Bosque S/N, 1900 La Plata, Argentina*
[9] *Instituto de Astrofísica de La Plata (CCT La Plata - CONICET - UNLP), Argentina*
[10] *Consejo Nacional de Investigaciones Científicas y Técnicas, Rivadavia 1917, C1033AAJ Ciudad Autónoma de Buenos Aires, Argentina*
[11] *Planetario "Galileo Galilei", Secretaría de Cultura, Ciudad Autónoma de Buenos Aires, Argentina*
[12] *Department of Physics and Astronomy, UNC-Chapel Hill, CB3255, Phillips Hall, Chapel Hill, NC 27599, USA*
[13] *Institute of Cosmology and Gravitation, Dennis Sciama Building, Burnaby Road, Portsmouth PO1 3FX, United Kingdom*
[14] *Department of Physics and Astronomy, Michigan State University, East Lansing, Michigan 48824, USA*

Какие они бывают…

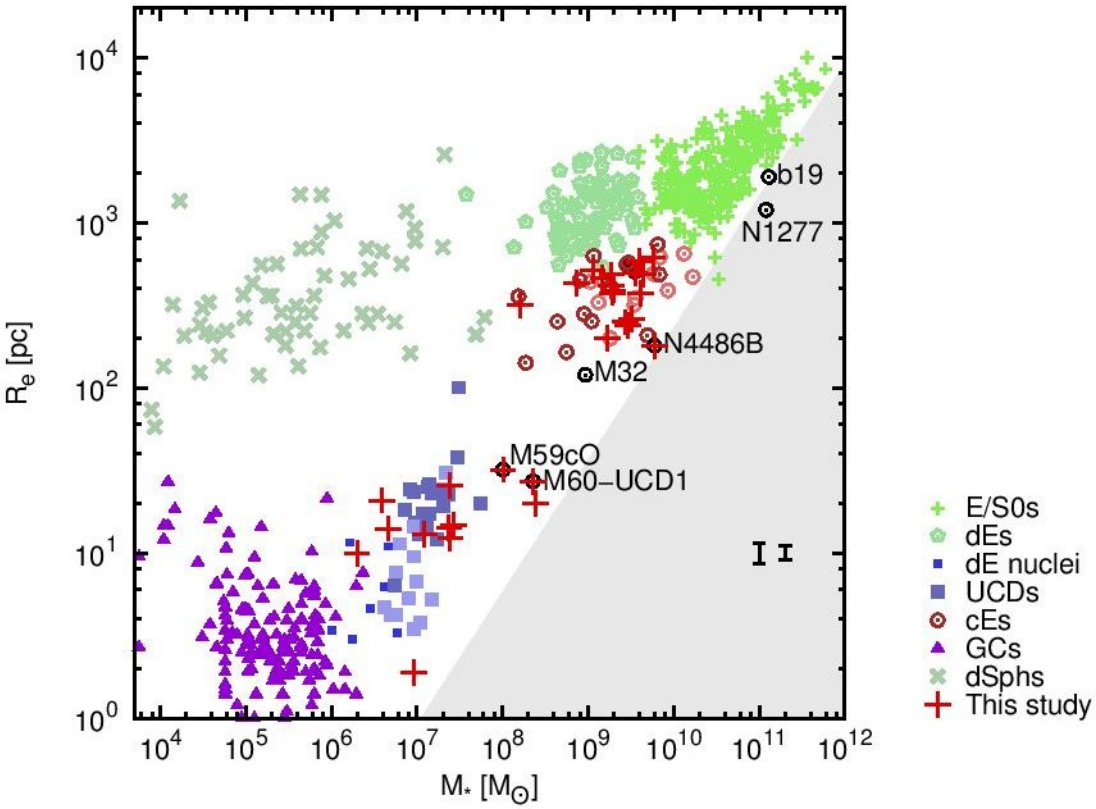

Какие у них металличности

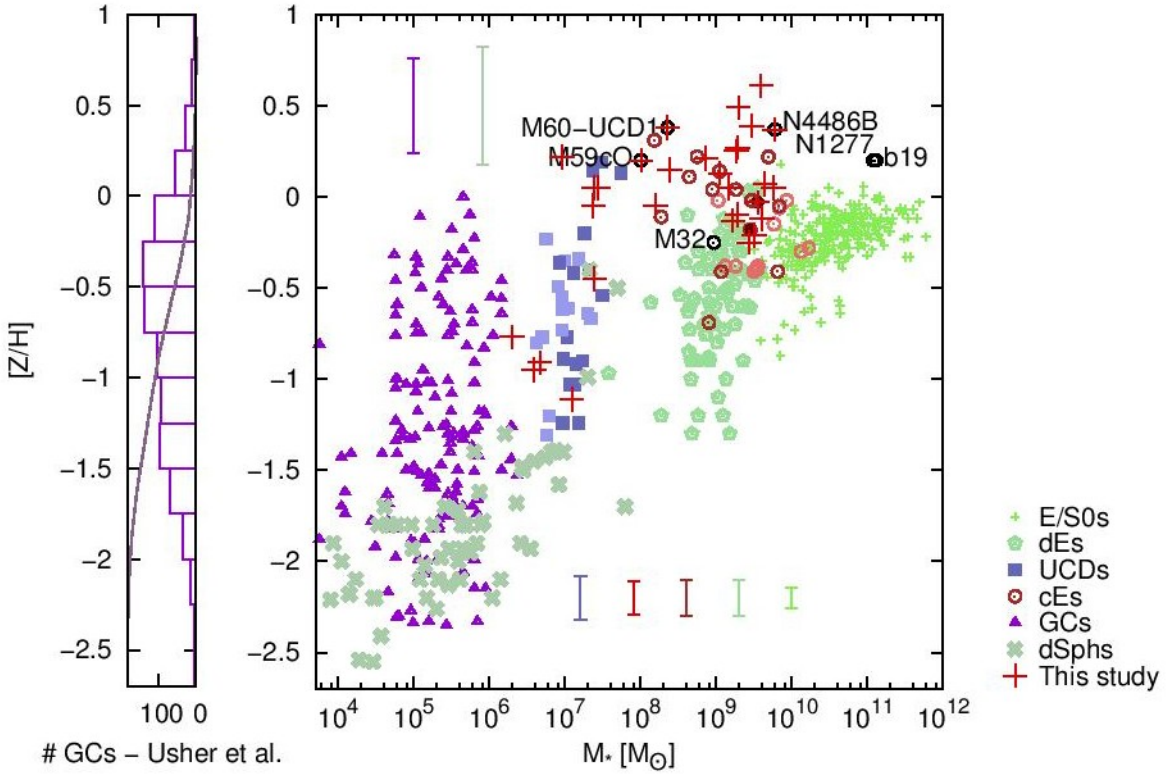

Какое у них все остальное

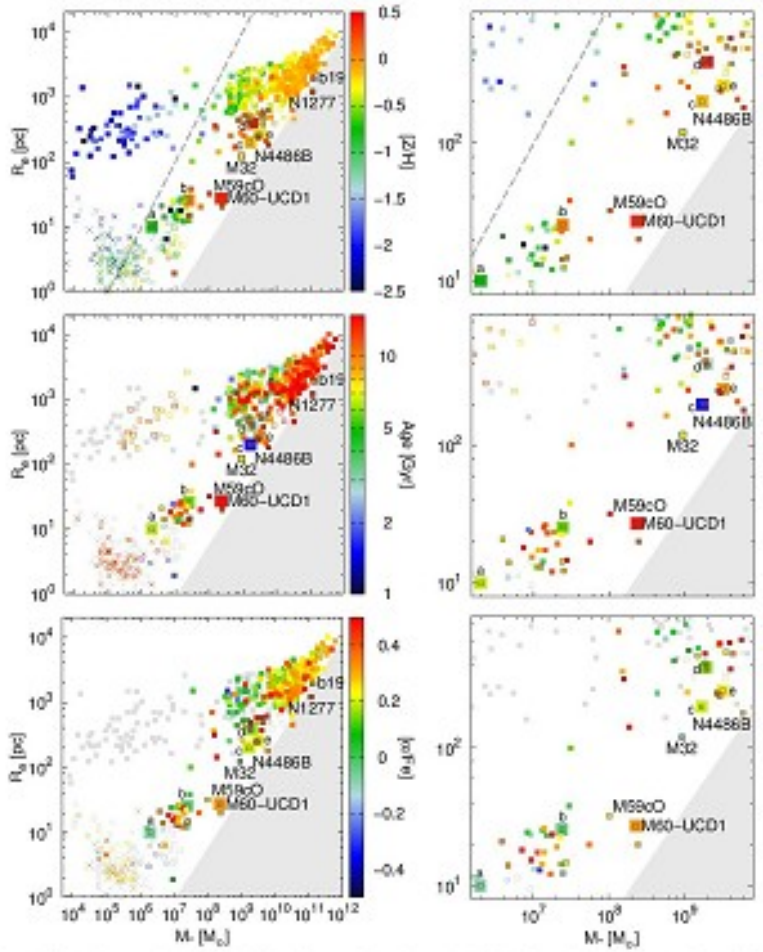

Figure 5. Size-stellar mass plots colour coded by stellar population characteristics. The colours display from top to bottom the SSP-equivalent metallicity, age, and [α/Fe]. The panels in the right column are zoom-ins to the parameter space of our CSSs. Globular clusters are displayed with crosses, dwarf nuclei with open circles, and the rest with squares. Literature CSSs without a measurement of [α/Fe] are shown with open squares. The ages of dSphs are also plotted with open squared, since they are mass-weighted averages, which are upper limits for the luminosity weighted ages. Objects with information lacking are plotted grey. The CSSs (our objects are highlighted with grey borders) exhibit metallicities that exceed those of other objects at the same mass. At low mass a number of them separate from globular clusters by exhibiting younger ages. The objects discussed in Section 5.1 are highlighted with large symbols (in order of increasing stellar mass: NGC 3628-UCD1 – a, NGC 4546-UCD1 – b, M60-UCD1, VCC 1615cE – c, and cE1 and cE2 from Huxor et al. 2011b – d,e). The grey dashed line in the middle panel is a line of constant velocity dispersion inferred from the virial theorem with constant virial coefficient.

Astro-ph: 1511.03275

THE AZIMUTHAL DEPENDENCE OF OUTFLOWS AND ACCRETION DETECTED USING O VI ABSORPTIO

GLENN G. KACPRZAK[1], SOWGAT MUZAHID[2], CHRISTOPHER W. CHURCHILL[3], NIKOLE M. NIELSEN[1], JANE C. CHARLTON[2]

ABSTRACT

We report a bimodality in the azimuthal angle (Φ) distribution of gas around galaxies traced by O VI absorption. We present the mean Φ probability distribution function of 29 *HST*-imaged O VI absorbing (EW>0.1 Å) and 24 non-absorbing (EW<0.1 Å) isolated galaxies ($0.08<z<0.67$) within $\sim$ 200 kpc of background quasars. We show that EW is anti-correlated with impact parameter and O VI covering fraction decreases from 80% within 50 kpc to 33% at 200 kpc. The presence of O VI absorption is azimuthally dependent and occurs between $\pm$10–20° of the galaxy projected major axis and within $\pm$30° of the projected minor axis. We find higher EWs along the projected minor axis with weaker EWs along the project major axis. Highly inclined galaxies have the lowest covering fractions due to minimized outflow/inflow cross-section geometry. Absorbing galaxies also have bluer colors while non-absorbers have redder colors, suggesting that star-formation is a key driver in the O VI detection rate. O VI surrounding blue galaxies exists primarily along the projected minor axis with wide opening angles while O VI surrounding red galaxies exists primarily along the projected major axis with smaller opening angles, which may explain why absorption around red galaxies is less frequently detected. Our results are consistent with CGM originating from major axis-fed inflows/recycled gas and from minor axis-driven outflows. Non-detected O VI occurs between Φ=20–60°, suggesting that O VI is not mixed throughout the CGM and remains confined within the outflows and the disk-plane. We find low O VI covering fractions within $\pm$10° of the projected major axis, suggesting that cool dense gas resides in a narrow planer geometry surrounded by diffuse O VI gas.

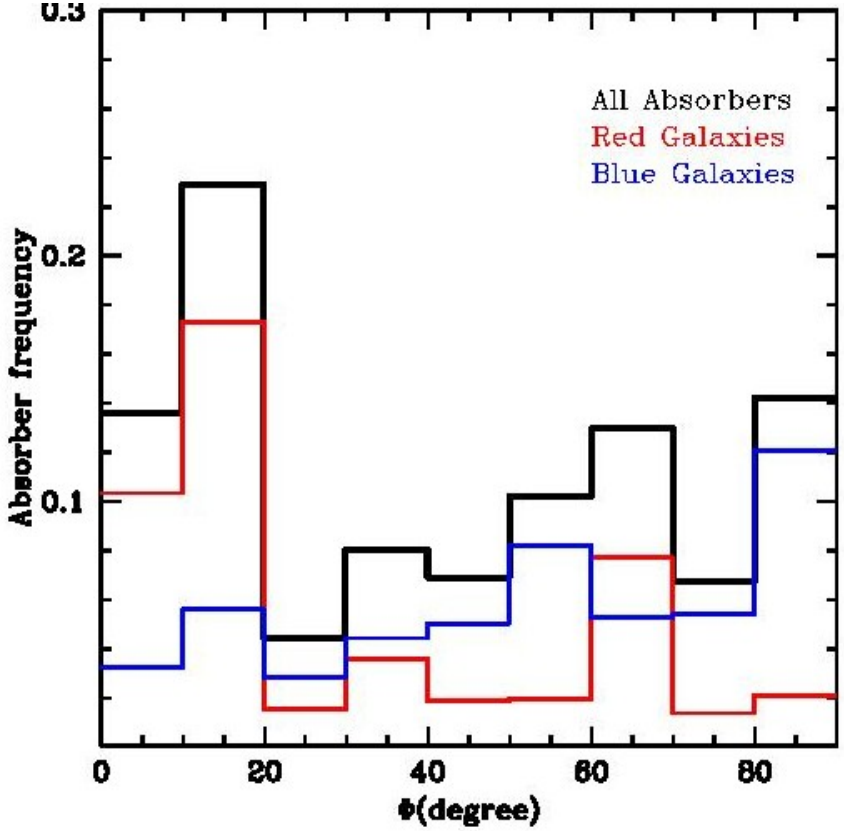

FIG. 8.— Φ distribution for absorbing galaxies from the top panel of Figure 4. We show the relative contributions of blue and red galaxies bifurcated at a $B-K$ and $u-r$ color of 1.5 (see Figure 7). Red galaxies show a preference along the projected major axis while blue galaxies prefer the project minor axis. This difference in orientation preference may explain why blue galaxies are more frequently detected as absorbers given the difference in opening angle between inflowing and outflowing gas.

Astro-ph: 1511.03499

No direct coupling between bending of galaxy disc stellar age and light profiles

T. Ruiz-Lara,[1,2⋆] I. Pérez,[1,2] E. Florido,[1,2] P. Sánchez-Blázquez,[3] J. Méndez-Abreu,[4] M. Lyubenova,[5] J. Falcón-Barroso,[6,7] L. Sánchez-Menguiano,[1,8] S. F. Sánchez,[9] L. Galbany,[10,11] R. García-Benito,[8] R. M. González Delgado,[8] B. Husemann,[12] C. Kehrig,[8] Ángel R. López-Sánchez [13,14] R. A. Marino,[15,16] D. Mast,[17,18] P. Papaderos,[19] G. van de Ven,[20] C.J. Walcher,[21] S. Zibetti,[22] and the CALIFA team

[1] *Departamento de Física Teórica y del Cosmos, Universidad de Granada, Campus de Fuentenueva, E-18071 Granada, Spain*
[2] *Instituto Carlos I de Física Teórica y computacional, Universidad de Granada, E-18071 Granada, Spain*
[3] *Departamento de Física Teórica, Universidad Autónoma de Madrid, E-28049 Cantoblanco, Spain*
[4] *School of Physics and Astronomy, University of St Andrews, SUPA, North Haugh, KY16 9SS St Andrews, UK*
[5] *Kapteyn Astronomical Institute, University of Groningen, PO Box 800, NL-9700 AV Groningen, the Netherlands*
[6] *Instituto de Astrofísica de Canarias, Calle Vía Láctea s/n, E-38205 La Laguna, Tenerife, Spain*
[7] *Departamento de Astrofísica, Universidad de La Laguna, E-38200 La Laguna, Tenerife, Spain*
[8] *Instituto de Astrofísica de Andalucía (CSIC), Glorieta de la Astronomía s/n, Aptdo. 3004, E-18080 Granada, Spain*
[9] *Instituto de Astronomía, Universidad Nacional Autónoma de México, A.P. 70-264, 04510 México D.F., Mexico*
[10] *Millennium Institute of Astrophysics, Santiago, Chile*
[11] *Departamento de Astronomía, Universidad de Chile, Camino El Observatorio 1515, Las Condes, Santiago, Chile*
[12] *European Southern Observatory (ESO), Karl-Schwarzschild-Str. 2, D-85748 Garching b. München, Germany*
[13] *Australian Astronomical Observatory, PO Box 915, North Ryde, NSW 1670,Australia*
[14] *Department of Physics and Astronomy, Macquarie University, NSW 2109, Australia*
[15] *CEI Campus Moncloa, UCM-UPM, Departamento de Astrofśica y CC. de la Atmósfera, Facultad de CC. Físicas, Universidad Complutense de Madrid, Avda. Complutense s/n, E-28040 Madrid, Spain*
[16] *Department of Physics, Institute for Astronomy, ETH Zürich, CH-8093 Zürich, Switzerland*
[17] *Observatorio Astronómico, Laprida 854, X5000BGR, Córdoba, Argentina*

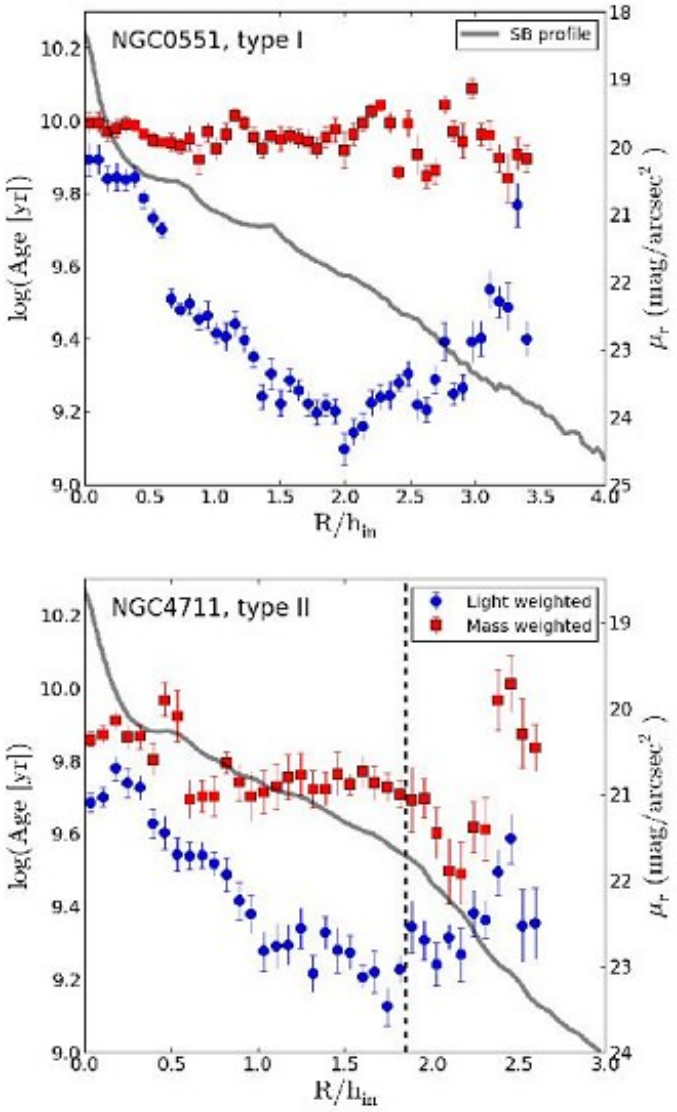

Figure 1. Age radial profile in logarithmic scale and surface brightness profile (SDSS r-band) for NGC 0551 (top panel, type I) and NGC 4711 (bottom panel, type II). Red (blue) squares (points) indicate mass-weighted (light-weighted) values. The black dashed line is located at the break radius. Grey continuous lines corresponds to the SB profiles (see right y-axis).